

Simplified relationships for estimating seismic slope stability

Ernesto Ausilio, Francesco Silvestri, Giuseppe Tropeano

Dipartimento di Difesa del Suolo, Università della Calabria, Arcavacata di Rende, Cosenza, Italy Author(s)

ABSTRACT

Eurocode 8 addresses seismic slope stability analysis with reference to limit state design, specifying a 50% reduction of the peak horizontal inertia force of a potentially sliding mass. Such a coefficient has been shown to depend on several factors, including soil deformability and the frequency content of the seismic action. In this paper the reduction coefficient is expressed with reference to the above factors and compared to EC8 provisions for all soil classes. A simplified design procedure is then suggested by referring to updated correlations based on the Newmark sliding block model, including the influence of amplitude, duration and mean period of the ground motion on the predicted displacement. The reduction coefficient is further generalised to account for the slope ductility, i.e. the capability of sustain prescribed threshold displacements. The whole procedure has been calibrated through analyses carried out using acceleration time histories, selected from a database of records of Italian seismic events, on typical subsoil layering pertaining to the EC8 classes, also adopted by the Italian seismic Code.

Keywords: slope stability, reduction coefficient, displacement-based design, simplified analysis

1 BACKGROUND

The conventional pseudo-static approach in the slope stability analysis considers an equivalent seismic force:

$$F_H = k_H \cdot W \quad (1)$$

where k_H is the seismic coefficient and W is the weight of the potentially sliding mass (Figure 1).

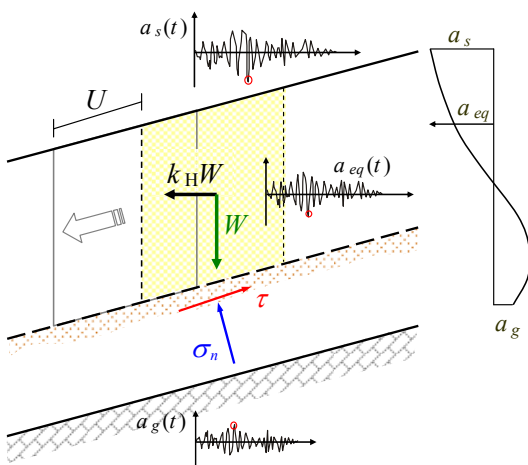


Figure 1. Sketch of the pseudo-static analysis of a slope.

In its most general meaning, the seismic coefficient should represent the resultant value of the non-uniform distribution of inertia forces in the subsoil above the sliding surface. Its value, expressed in g's, corresponds to an 'equivalent acceleration', a_{eq} , i.e. the peak amplitude of an 'equivalent accelerogram' acting on the slope.

In an infinite slope model (see Fig. 1), which is a good approximation if the effects of 2D propagation and the surface topography can be neglected, the equivalent acceleration can be expressed as:

$$a_{eq} = \alpha \cdot a_s \quad (2)$$

where α is a reduction factor of the peak surface acceleration, a_s , which should account for:

- the deformability of the subsoil with respect to the characteristic wavelengths of the seismic shaking;
- the ductility of the sliding mass, intended as its capability to sustain permanent displacements.

Eurocode 8 (prEN1998-5, 2003) prescribes to compute the equivalent seismic action by assuming:

$$k_H = 0.5 \cdot S \cdot \frac{a_g}{g} \quad (3)$$

where S is the surface amplification factor of a_g , the peak ground acceleration on outcropping bedrock.

By comparing eqs. (2) and (3), the EC8 approach corresponds to assume $\alpha=0.5$, so that:

$$a_{eq} = 0.5 \cdot S \cdot a_g \quad (4)$$

For the soil parameter S , EC8 (prEN 1998-1, 2003) specifies constant values associated to the subsoil class as listed in Table 1. In the first draft of the forecoming Italian seismic code (OPCM, 2003) the parameter S attributed to soil classes B, C, E assumes the common value of 1.25 (cf. Tab. 1).

Table 1. Constant soil amplification factors.

Subsoil class	S -EC8 (2003)	S -OPCM (2003)	S -ETC12 (2006)	
	A	A	A1	1.00
B	1.20	1.25		1.30
C	1.15	1.25		1.15
D	1.35	1.35		1.10
E	1.40	1.25		1.35

In a recent proposal of reviewing EC8, ETC12 (2006) suggests different values for S (Tab. 1), to be referred to a more complete re-classification of soil types according to the equivalent shear wave velocity, $V_{S,30}$, and the bedrock depth, H . Such reclassification, synthesized in Figure 2, introduces two sub-classes, A1 and A2, for the stiffer soils.

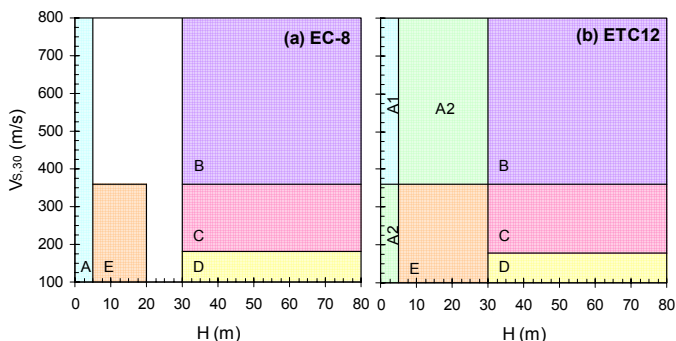


Figure 2. Soil classification by (a) EC8 and (b) ETC12.

It is well known, however, that the surface amplification is influenced by the non-linear soil behaviour (Seed et al., 1976), and this should be accounted for the slope stability analyses (Bray et al., 1998). In a recent work by the Authors (Ausilio et al., 2007), one-dimensional seismic site response (SSR) analyses were carried out on a set of ‘virtual’ subsoil models corresponding to the updated classification suggested by ETC12 (2006), with an accelerometric database representative of the Italian seismicity (Scasserra et al., 2006). The data processing led to the average curves in Figure 3; these express, for each subsoil class, the non-linear response factor (computed as a_s/a_g and denoted as S_{NL} hereafter) as a power law function of the reference ground acceleration a_g (Table 2).

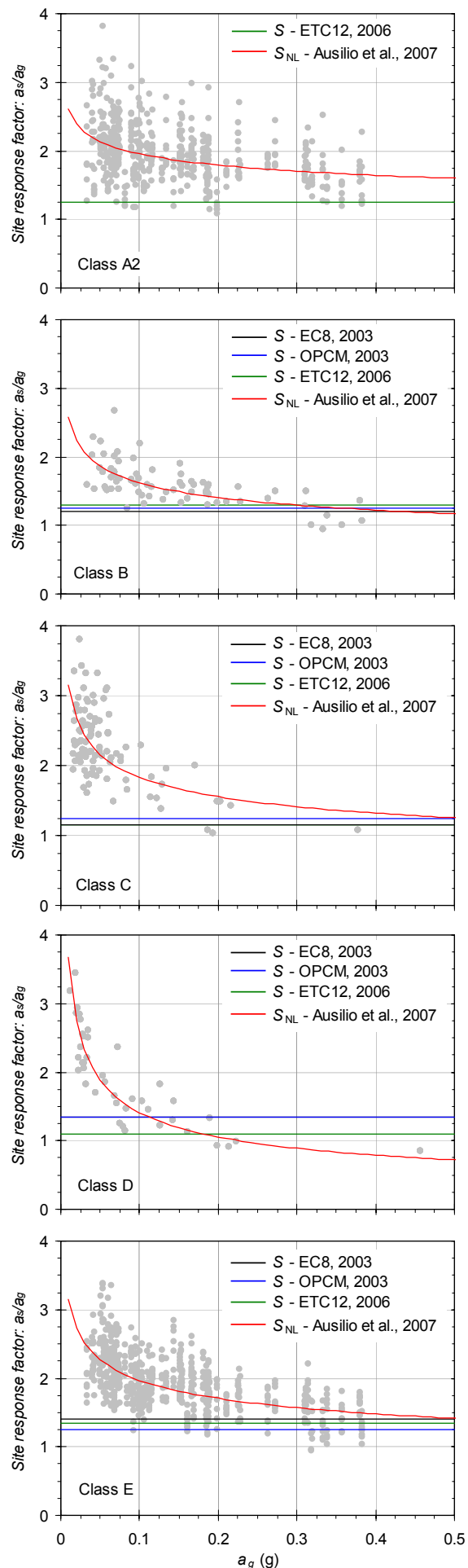


Figure 3. Data points and best fit curves of the non-linear response factor compared to the constant values suggested by EC8 and updated by OPCM (2003) and ETC12 (2006).

Table 2. Non-linear soil amplification factors by Ausilio et al. (2007).

Subsoil class	$S_{NL} = p \cdot a_g^m$		
	p	m	R^2
A1	1	0	-
A2	1.466	-0.125	0.1397
B	1.018	-0.202	0.4506
C	1.062	-0.236	0.3906
D	0.539	-0.417	0.8477
E	1.227	-0.205	0.3971

From the plots and the values of the power law parameters, it is apparent that the degree of non-linear dependence of S_{NL} on a_g increases with the soil deformability (class A2 to D). The comparison between linear and non-linear soil factors in Fig. 3 highlights that, except for class D, the codes indications correspond to about the lower bound of the analytical data and of the curves $S_{NL}:a_g$.

With reference to the above framework, in the following three different types of reduction factors will be introduced and discussed:

- the ‘frequency reduction factor’, α_F , as a function of soil deformability (subsoil classes), expressed as the ratio of the fundamental subsoil period to the mean period of acceleration time history;
- the ‘displacement reduction factor’, α_U , expressed with reference to the slope ductility, and depending on a design limiting value of the permanent displacement;
- the ‘global reduction factor’, α_{FU} , which considers simultaneously both the above features.

2 THE FREQUENCY REDUCTION FACTOR α_F

Following the approach suggested by Bray et al. (1998), a reduction factor, α_F , which takes into account the soil deformability only, can be defined as a function of the ratio between the fundamental subsoil period, T_s , and the mean period of the acceleration time history, T_m . Such ratio is conceptually equivalent to the frequency factor corresponding to the first resonant mode of an ideal subsoil. Referring to the dynamic equilibrium of a soil column, Ausilio et al. (2007) computed, for the same set of SSR analyses used to derive the expressions of S_{NL} , the values of a_{eq} from the shear stress time history, $\tau(t)$, and the total vertical stress, σ_v , evaluated to the depth H of a possible sliding surface:

$$a_{eq} = \max \left[\frac{\tau(H, t)}{\sigma_v(H)} \cdot g \right] = \frac{\tau_{\max}(H)}{\sigma_v(H)} \cdot g \quad (5)$$

All the data sets relevant to the different soil classes were seen to yield practically the same trend of the deformability reduction factor; as a consequence, they have been grouped together (Figure 4) and statistically processed to obtain the median curve:

$$\alpha_F = 0.4199 \cdot \left(\frac{T_s}{T_m} \right)^{-0.815} \quad (6)$$

which is plotted in Figure 4 together with those relevant to probability of exceedance equal to 16% and 84%.

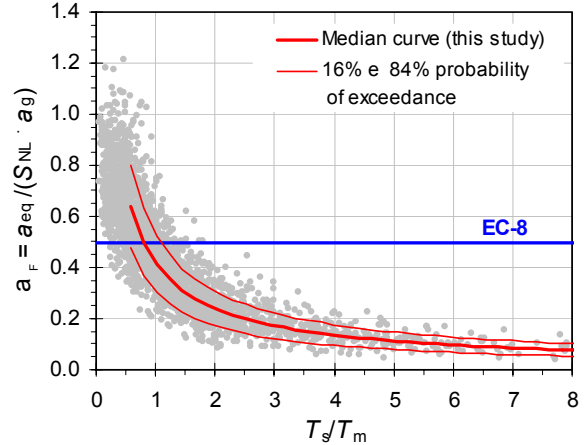


Figure 4. Reduction of equivalent acceleration with the period ratio.

It can be noted that, for $T_s/T_m < 1$, the upper bound reduction factor α_F results greater than 0.5 (i.e. the value specified by EC8), decreasing even down to 0.1 for the highest T_s/T_m values considered. The high values of α_F in the range of low period ratio should be attributed to resonance at the first vibration modes for relatively stiff subsoils with a marked non-linear behaviour. For the cases when $T_s > T_m$, where the response of a deformable subsoil is affected by asynchronous motion and resonance at higher modes, EC8 specifies more conservative predictions than those obtained in this study.

Figure 5 reports the comparison between the values of the equivalent acceleration specified by EC8 (eq. 4) and that resulting from the present study as:

$$a_{eq} = \alpha_F \cdot a_s = \alpha_F \left(\frac{T_s}{T_m} \right) \cdot S_{NL}(a_g) \cdot a_g \quad (7)$$

using either the median or the upper bound curve in Fig. 4 for α_F . The results again show that the EC8 provisions are as more conservative as soil deformability and seismic action increase.

3 THE DISPLACEMENT CORRELATIONS

The statistical correlations based on the Newmark sliding block model express the dependency of the permanent displacement of a rigid slope, U , on the ratio, η , between the critical acceleration, a_y , which brings the slope to a prescribed limit state, and a given value of the peak acceleration, a_{max} . This latter can be taken equal either to a_g , or to a_s , or to a_{eq} , ac-

cording to the approach followed to describe the relevant seismic motion.

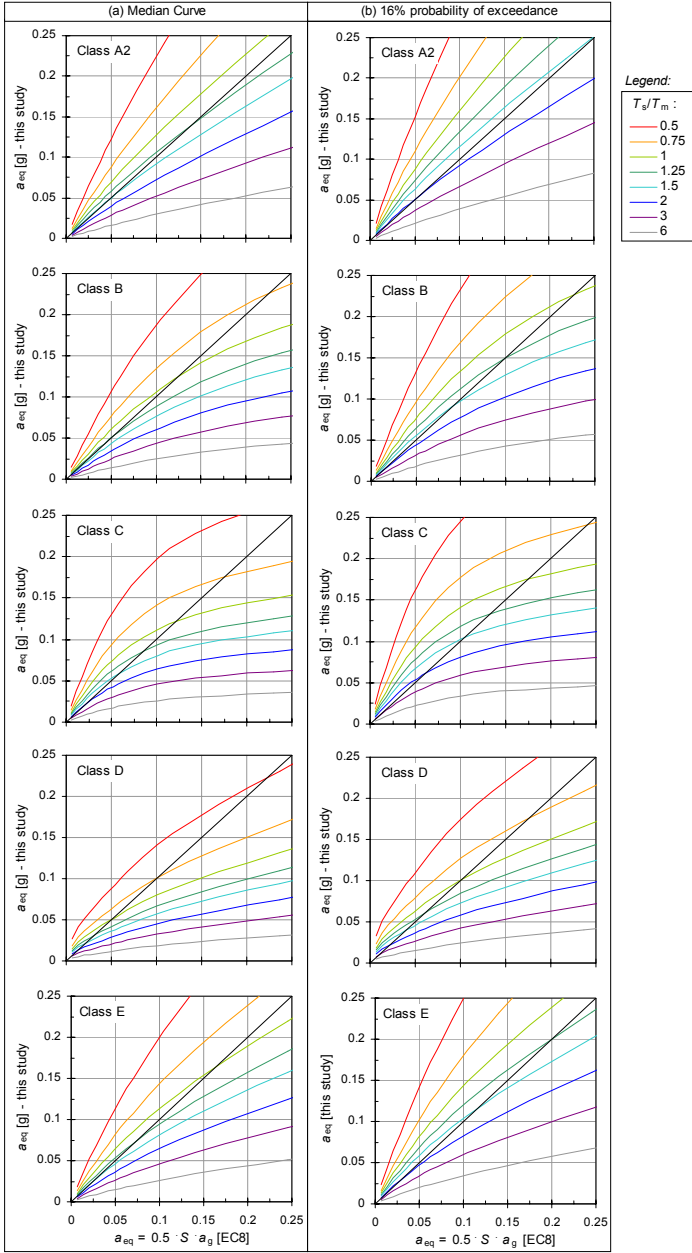


Figure 5. Comparison between the equivalent acceleration obtained using the procedure of Ausilio et al. (2007) and that specified by EC8.

Ausilio et al. (2007) developed such statistical correlations based on the regression analysis of 318 Newmark displacement values from Italian selected accelerograms and values of $\eta = a_y/a_{\max}$ varying from 0.1 to 0.9. If the displacement U is divided by a_{\max} , the correlation shows a significant scatter and a consistent dependency on the product between the mean period (T_m) and the significant duration (D_{5-95}) of the accelerogram, as shown by Figure 6. The same figure also reports the sampling distribution of $T_m D_{5-95}$ of the accelerogram subsets, represented with box plots using different colors.

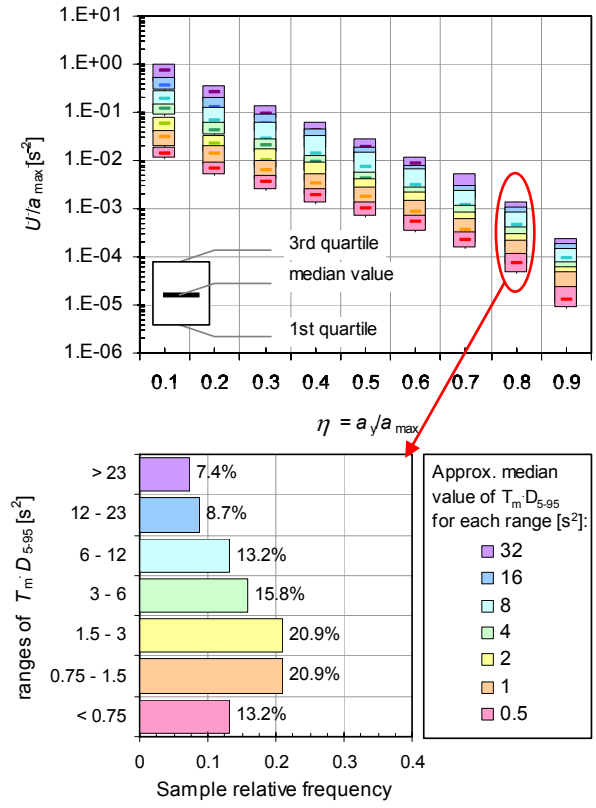


Figure 6. Variation of displacement correlation with the product between mean period and significant duration.

Therefore, the statistical processing of the same data was reviewed looking for a rational normalisation criteria, with the aim to obtain a lower data dispersion. From the analytical solution of the rigid block model subjected to a simple harmonic accelerogram with peak amplitude a_{\max} , duration D_{5-95} and period T_m , it results that the displacement, after normalization by the product $a_{\max} D_{5-95} T_m$, results a function of the only acceleration ratio η (Yegian et al, 1991).

The statistical analysis showed that each series of normalized displacement samples could be interpreted with lognormal distribution. The regression curves relevant to the different percentiles were obtained by different analytical models. The simplest is a linear function (in semi-logarithmic scale) described by (Figure 7a):

$$\log\left(\frac{U}{a_{\max} \cdot T_m \cdot D_{5-95}}\right) = -1.349 - 3.410 \cdot \frac{a_y}{a_{\max}} + \sigma \cdot t \quad (8)$$

where σ is the standard deviation (0.35 in \log_{10} units) and t is the inverse Normal standard distribution for a generic design level of probability.

A non-linear function, based on the approach followed by Ambraseys & Menu (1988), was also tested (Figure 7b). The resulting relationship is the following:

$$\log\left(\frac{U}{a_{\max} \cdot T_m \cdot D_{5-95}}\right) = -2.571 + 2.389 \cdot \log(1-\eta) - 1.125 \cdot \log(\eta) + \sigma \cdot t \quad (9)$$

where, again, $\sigma = 0.35$. The regression coefficients, R^2 , for the relationships (8) and (9) on the median sample values resulted 0.969 and 0.999, respectively. The better overall response of the non-linear regression at the different acceleration ratios and displacement percentiles is well readable in Figure 7.

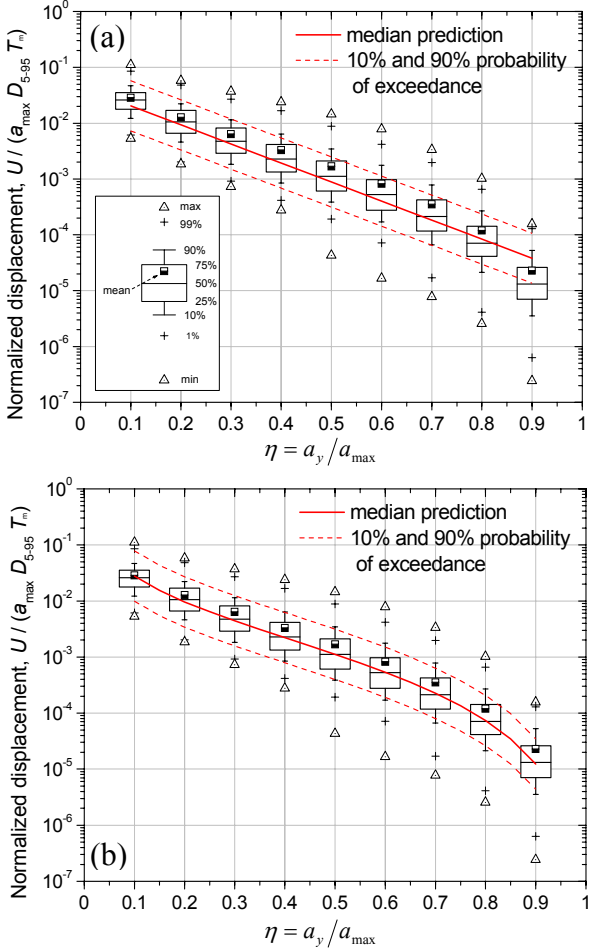


Figure 7. Statistical processing of displacements and comparison between linear (a) and non linear (b) regression curves.

4 THE DISPLACEMENT REDUCTION FACTOR α_U

For a rigid slope model which can sustain a displacement threshold value, u_{amm} (Biondi et al., 2007), in eqs. (8)-(9) it can be assumed $a_{\max} = a_g$ and $a_y = a_{\lim}$. For instance, eq. (8) becomes:

$$\log\left(\frac{u_{amm}}{a_g \cdot T_m \cdot D_{5-95}}\right) = -1.349 - 3.410 \cdot \frac{a_{\lim}}{a_g} + \sigma \cdot t \quad (10)$$

Therefore, the displacement reduction factor, α_U , results from the probability that the seismic slope displacement, U , is greater than u_{amm} (Rampello et al.,

2006). Such probability is theoretically conditioned on the variables a_{\max} , η and the product $T_m \cdot D_{5-95}$. In this study, all these random variables were considered as deterministic, so that the probability was only dependent on the statistical distribution of the normalized displacement. Fixing an exceedance probability of 10% (i.e. $\sigma \cdot t = 0.35 \cdot 1.281$), and manipulating eq. (10), the expression of the displacement reduction coefficient, α_U , is obtained as:

$$\alpha_U = \frac{a_{\lim}}{a_g} = \frac{1}{3.410} \cdot \left[-0.901 - \log\left(\frac{u_{amm}}{a_g \cdot T_m \cdot D_{5-95}}\right) \right] \quad (11)$$

Summarising, this coefficient represents the factor by which the reference ground motion amplitude (a_g) needs to be reduced, to yield an equivalent acceleration (a_{\lim}) associated with a limit state defined by u_{amm} (Biondi et al., 2007), accounting for the ductility of a rigid slope which can slide along a critical surface. In other words, a_{\lim} is the acceleration amplitude that theoretically brings the slope to a given threshold displacement u_{amm} , with the a selected design probability of exceedance. The ratio between a_{\lim} and actual slope yield acceleration, a_y , is an index of the slope safety factor.

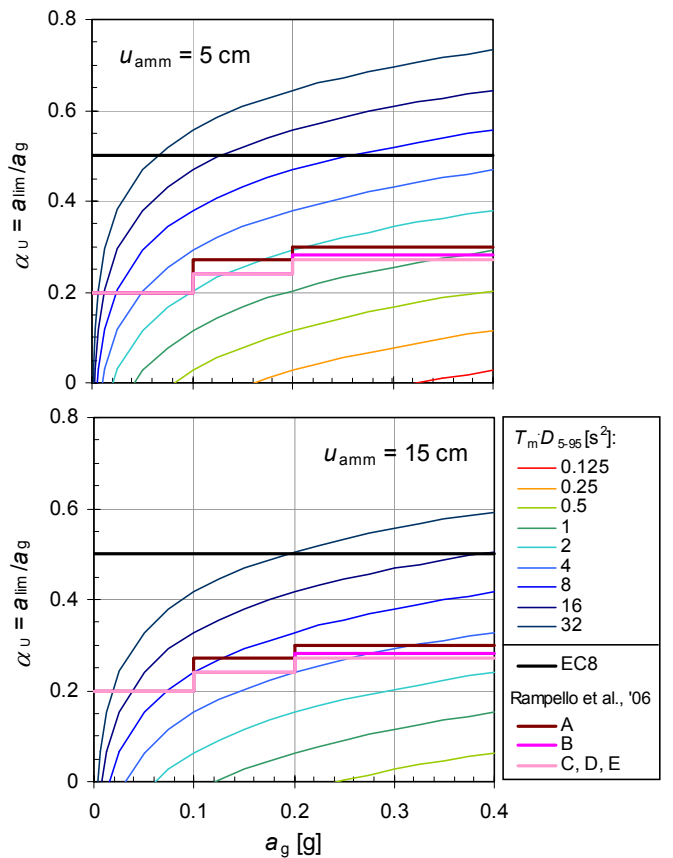


Figure 8. Displacement reduction factor α_U as a function of the peak ground acceleration and the product of seismic motion parameters, for two values of threshold displacements.

Figure 8 shows the dependency of coefficient α_U on a_g and $T_m \cdot D_{5-95}$, computed by eq. (11) with reference to two threshold displacements, 5 and 15 cm. The constant reduction factor specified by EC8 results

generally conservative for the most frequent values of $T_m \cdot D_{5-95}$. The figure also reports the values computed by Rampello et al. (2006), with reference to the same Italian seismic database, and again with 10% probability of exceedance. Note that they are characterised by a stepwise increase with a_g depending on the soil class, and that plot around the average of those from this study.

In Figure 9 the values by Rampello et al. (2006), which were obtained for limit states between 10 and 15 cm, are again compared to those obtained in this study at displacements from 5 to 15 cm, for the product of the seismic motion parameters $T_m \cdot D_{5-95}$ equal to the median value of the dataset (2.5 s^2). The data show an overall agreement for a_g higher than 0.2 g , while those obtained in this study appear increasingly lower at weak ground motion amplitudes.

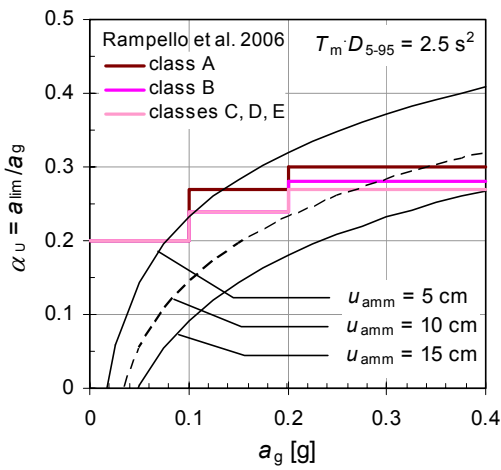


Figure 9. Comparison between the reduction factors proposed by Rampello et al. (2006) and the median values obtained in this study.

5 THE GLOBAL REDUCTION FACTOR α_{FU}

The above described approach can be extended accounting also for the deformability effects on the definition of a_{lim} . For instance, inverting eq. (11) as:

$$a_{lim} = \frac{a_g}{3.410} \cdot \left[-0.901 - \log\left(\frac{u_{amm}}{a_g \cdot T_m \cdot D_{5-95}}\right) \right] \quad (12)$$

the definition of a_{lim} can be re-formulated more generally, by replacing a_g in eq. (12) with the value of a_s given by eq. (7), obtaining:

$$a_{lim}^* = \frac{\alpha_F S_{NL} a_g}{3.410} \cdot \left[-0.901 - \log\left(\frac{u_{amm}}{\alpha_F S_{NL} a_g \cdot T_m \cdot D_{5-95}}\right) \right] \quad (13)$$

and then the expression for the ‘global reduction factor’ α_{FU} as:

$$\alpha_{FU} = \frac{a_{lim}^*}{a_g} = \frac{\alpha_F S_{NL}}{3.410} \cdot \left[-0.901 - \log\left(\frac{u_{amm}}{\alpha_F S_{NL} a_g \cdot T_m \cdot D_{5-95}}\right) \right] \quad (14)$$

Due to the dependency of α_F on the period ratio, T_s/T_m (eq. 6), it is rather complicated to compare the above expression with codes and literature studies. Therefore, maintaining the simplified and conservative character of the procedure, it is possible to introduce an upper bound value of α_F (e.g. 0.7, that corresponds to the median curve in Fig.4 for $T_s/T_m = 0.5$), obtaining:

$$\alpha_{FU} = \frac{a_{lim}^*}{a_g} = \frac{0.7 \cdot S_{NL}}{3.410} \left[-0.901 - \log\left(\frac{u_{amm}}{0.7 \cdot S_{NL} \cdot a_g \cdot T_m \cdot D_{5-95}}\right) \right] \quad (15)$$

In Figure 10, the coefficient α_{FU} obtained from eq. (15) for subsoil type E is compared, for two displacement values, with the relationship suggested by Stewart et al. (2003) at the same 10% probability of exceedance. Both the prediction refer to $T_m = 0.4 \text{ s}$, i.e. the average value of mean period of the accelerometric database used in this study.

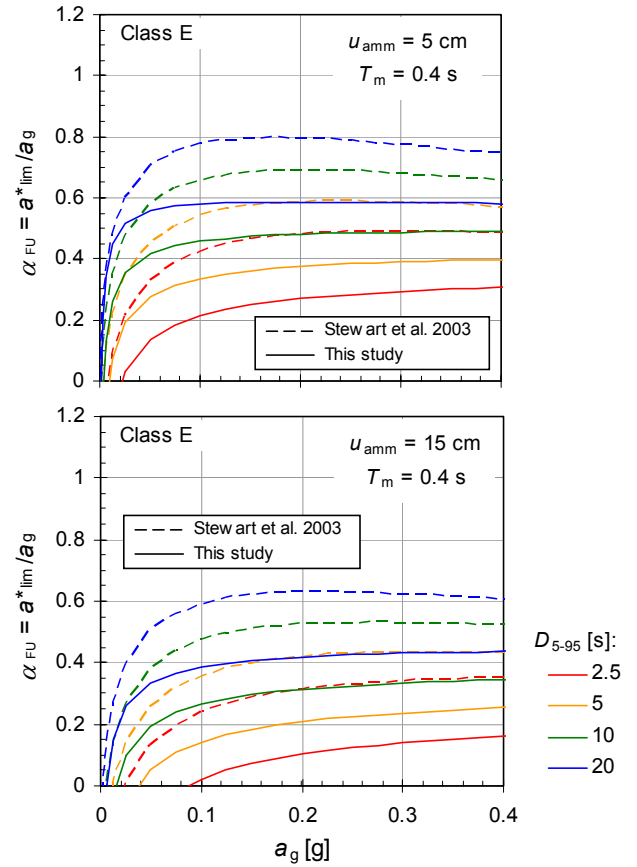


Figure 10. Comparison between the reduction factors, including deformability effects, proposed by Stewart et al. (2003) and the relationships obtained in this study for subsoil class E.

It must be remarked that Stewart et al. (2003) evaluated the probability as the combination of statistical distribution of displacements and the estimate of duration using the attenuation law of Abrahamson and

Silva (1998). The same authors recommended to use the median value of combined distribution as the most significant in the return period considered (typically 475 years).

Figure 11 shows a last comparison of the global reduction coefficient with the indications by EC8 and Rampello et al. (2006), again referring to the median value of the product $T_m \cdot D_{5-95}$ such as in Fig. 9. Note that, for $a_g > 0.15g$, the reduction factors computed in this study tend to approximate constant values, which are on the average about 50% those specified by EC-8 for u_{amm} of the order of 10cm. The lowest values of α_{FU} pertain to class D, for which it is expected the maximum reduction for deformability.

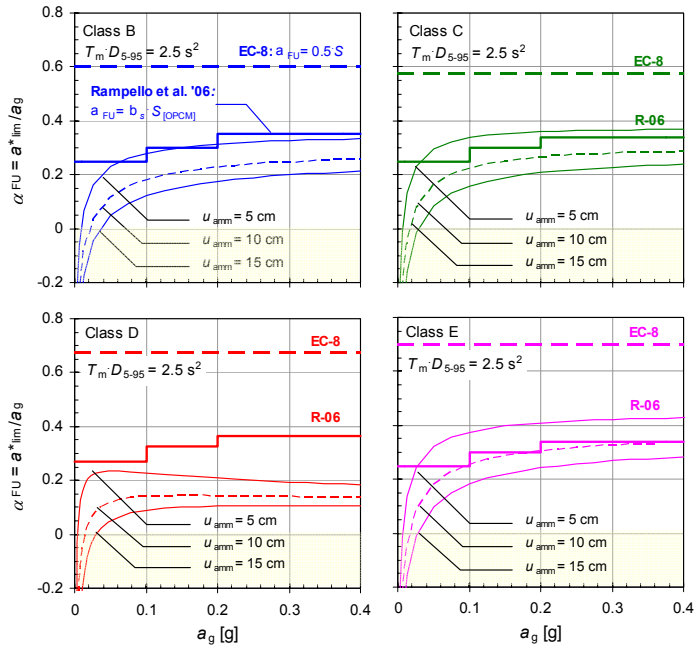


Figure 11. Comparison between the global reduction factor, including ductility and deformability, with the EC-8 provisions including site effects, and the values proposed by Rampello et al 2006 (R-06), for all subsoil classes.

6 CONCLUSIONS

Three approaches were described for the reduction of seismic coefficient for pseudo-static analyses of gentle slopes. They were all based on statistical analyses of the dynamic response of virtual subsoils subjected to seismic records representative of Italian seismicity. All the approaches resulted mostly less conservative than EC8 provisions.

The first approach only considers the effects of soil deformability. This method needs the determination of the fundamental period of the sliding mass, which can be either directly measured (e.g. by passive geophysical tests) or obtained from the shear wave velocity profile and the location of the possible sliding surface. The use of this method can be hampered by the need to estimate the mean earthquake period.

The second method assumes a rigid slope model and it is based only on the assumption of a threshold displacement and the evaluation of the product $T_m \cdot D_{5-95}$. These ground motion parameters can be obtained through statistical interpretations of seismic databases or, hopefully, using specific and reliable attenuation laws.

The third approach combines deformability and ductility, and should ideally need all the above mentioned soil and earthquake parameters. It must be highlighted that the combined effects of ductility and deformability can't be expressed using uncoupled individual coefficients.

All of the above methods can be addressed by EC8, NADs, and national codes, provided that more specific indications are given on the choice of the limit displacement values.

7 ACKNOWLEDGMENTS

This work is a part of a Research Project funded by ReLUIS (Italian University Network of Seismic Engineering Laboratories) Consortium. The Authors wish to thank the coordinator, prof. Sebastiano Rampello, for his continuous support and the fruitful discussions. The strong motion database used in this study was developed as part of an ongoing joint project involving researchers from the University of Rome La Sapienza and the University of California, Los Angeles, with support from the Pacific Earthquake Engineering Research Center.

REFERENCES

- Abrahamson, N.A. and Silva, W.J. 1996. Empirical Ground Motion Models. *Report prepared for Brookhaven National Laboratory*, New York, NY, May, 144p.
- Ambraseys, N.N. and Menu, J.M. 1988. Earthquake-induced ground displacements. *Earthquake Engineering and Structural Dynamics*, Vol. 16: 985-1006.
- Ausilio, E. Silvestri, F. Troncone, A. Tropeano, G. 2007. Seismic displacement analysis of homogeneous slopes: a review of existing simplified methods with reference to Italian seismicity. *IV International Conference on Earthquake Geotechnical Engineering*, Thessaloniki, Greece, June 25-28, 2007. ID 1614.
- Biondi , G. Cascone, E. Rampello S. 2007. Performance-based pseudo-static analysis of slopes. *IV International Conference on Earthquake Geotechnical Engineering*, Thessaloniki, Greece, June 25-28, 2007. ID 1645.
- Bray, J.D. Rathje, E.M. Augello, A.J. and Merry, S.M. 1998. Simplified Seismic Design Procedure for Geosynthetic-Lined. *Solid-Waste Landfills, Geosynthetics International*, 5(1-2), 203-235.
- prEN 1998-1, 2003. Eurocode 8: Design of structure for earthquake resistance,. Part 1: General rules, seismic actions and rules for buildings. CEN European Committee for Standardisation, Bruxelles, Belgium.
- prEN 1998-5, 2003. Eurocode 8: Design of structure for earthquake resistance,. Part 5: Foundations, retaining structures

and geotechnical aspects. CEN European Committee for Standardisation, Bruxelles, Belgium.

ETC12, 2006. General Report (ed. G. Bouckovalas), Workshop of ETC12 Evaluation Committee for the Application of EC8, Athens, Greece.

Lanzo, G. 2006, Database di accelerogrammi naturali italiani. *Report of Task 6.3 'Slope stability'*, ReLUIS Consortium (in italian).

Rampello S., Callisto L., Fargnoli P. 2006. Valutazione del coefficiente sismico equivalente. *Report of Task 6.3 'Slope stability'*, ReLUIS Consortium (in italiano).

Scasserra G., Lanzo G., Mollaioli F., Stewart J.P., Bazzurro P., and Decanini L.D. 2006. Preliminary comparison of ground motions from earthquakes in Italy with ground motion prediction equations for active tectonic regions, Proc. of 8th U.S. National Conference on Earthquake Engineering, San Francisco.

Seed, H.B. Murarka, J. Lysmer J. Idriss, I.M. 1976. Relationships between maximum acceleration, maximum velocity, distance from source and local site conditions from moderately strong earthquakes. Bull, Seism. Soc. Of America, Vol. 66, n. 4.

Stewart, J.P. Blake, T.M. and Hollingsworth, R.A. 2003. A screen analysis procedure for seismic slope stability, *Earthquake Spectra*, 19, 697–712.

Yegian, M.K. Marciano E.A. and Gharaman V.G. 1991. Earthquake-induced permanent displacement deformations: probabilistic approach. *Journal of Geotechnical Engineering*, ASCE, 117(1), pp. 35-50.